Journal of Computational and Applied Mathematics 236 (2012) 4181–4192

Contents lists available at SciVerse ScienceDirect

Journal of Computational and Applied Mathematics

journal homepage: www.elsevier.com/locate/cam

An accurate finite-difference method for ablation-type Stefan problems

S.L. Mitchell *, M. Vynnycky

Mathematics Application Consortium for Science and Industry (MACSI), Department of Mathematics and Statistics, University of Limerick, Limerick, Ireland

ARTICLE INFO

Article history:
Received 25 May 2011
Received in revised form 2 April 2012

Keywords:
Ablation
Stefan problem
Keller box scheme
Boundary immobilization
Starting solutions

ABSTRACT

A recently derived numerical algorithm for one-dimensional time-dependent Stefan problems is extended for the purpose of solving one-phase ablation-type moving boundary problems; in tandem with the Keller box finite-difference scheme, the so-called boundary immobilization method is used. An important component of the work is the use of variable transformations that must be built into the numerical algorithm in order to preserve second-order accuracy in both time and space. The analysis also determines that the ablation front initially moves as the time raised to the power 3/2; hence, it evolves considerably more slowly than the phase-change front in the classical Stefan problem with isothermal cooling.

1. Introduction

Ablation is the generic term used to denote the removal of material from the surface of an object by vaporization, chipping, or other erosive processes [1]. The term occurs in spaceflight associated with atmospheric reentry [2], the burning up of meteorites [3], the melting or sublimation of a solid [4], laser drilling in metals and the cornea [5], the reduction of glaciers by erosion [6] and the surgical removal of a body part or tissue, such as in atrial fibrillation [7]. In mathematical terms, ablation is one type of phase-change, or Stefan problem, i.e. a moving boundary problem in which the location of the surface of the ablating material is not known beforehand, but must be determined as part of the solution.

As with most Stefan problems, it is common to have to apply numerical methods in order to solve ablation-type problems. Probably the first to do so was Landau [8], who proposed an idealized ablation problem for the case of a semi-infinite melting solid with constant thermal properties, and solved it using numerical integration. Later, Goodman [9] applied the standard heat balance integral method (HBIM) to this problem and obtained adequate agreement with the ablation rate obtained by Landau [8]. Zien [10] adapted the standard HBIM by employing an exponential temperature profile. His results show better agreement with Landau's numerical result for the ablation rate than the standard HBIM. More recently, Braga et al. [11–13] have adapted the standard HBIM approach by assuming that the approximating temperature function is again a polynomial, but with its order determined by comparing the time ablation commences with standard exact analytical solutions for the pre-ablation stage. Mitchell & Myers [14,15], Mitchell [16] and Myers [17] have also applied HBIMs with polynomial temperature profiles to this problem, with the exponent determined as part of the solution process, but without relying on any exact solutions. This leads to significantly more accurate results than all previous heat balance integral methods. Yang et al. [18] have also applied the HBIM to ablation of a two-layer composite using a quadratic polynomial profile. On a few occasions, methods other than the HBIM have been employed. In [19,20], enthalpy formulations were used: Storti [19] developed a fixed domain numerical scheme, and solved the resulting equations using finite element methods; Wong & Walton [21] solved the single-phase semi-infinite laser ablation problem also by using a fixed grid, but with a volume-based finite difference approach. Other authors have used finite control volume procedures [22,23], whereas yet others have used finite difference methods [20].

* Corresponding author. Tel.: +353 61 202259.
E-mail address: sarah.mitchell@ul.ie (S.L. Mitchell).

0377-0427/$ – see front matter © 2012 Elsevier B.V. All rights reserved.
doi:10.1016/j.cam.2012.05.011

In spite of much activity, several shortcomings can be identified in the numerical solution of ablation problems. All solutions employing the HBIM require assumptions to be made on the form of the temperature profile; hence, it is not possible, in general, to give a quantitative estimate for the accuracy of a solution. As for all the other methods, although their order of accuracy is well-known when they are applied to non-moving boundary problems, extra care is necessary when moving boundaries are involved because iteration is necessary in order to find the location of the moving front; as far as we are aware, no formal verification of accuracy has been carried out for numerically-obtained solutions to ablation-type problems. The purpose of this paper therefore is to provide a numerical scheme which solves ablation-type problems with determinable accuracy.

In recent work [24,25], the boundary immobilization method coupled to a Keller Box finite difference discretization scheme was applied to two different one-phase one-dimensional time-dependent Stefan problems, and shown to give numerical solutions that are second-order accurate in time and space variables; in this respect, the algorithms are more accurate than earlier ones for either type of problem. At first sight, ablation-type problems may seem numerically no harder than the ones considered in [24,25]. However, as this paper will demonstrate, there are variety of new issues that need to be resolved in order to produce a numerical scheme that is second-order accurate in both time and space. First of all, unlike in the problems solved in [24,25], phase change does not necessarily start instantaneously, and subsidiary analysis turns out to be necessary in order to determine when and how the moving front develops; indeed, it proves essential to implement this into the solution algorithm in order to preserve numerical accuracy. A related issue is whether all the variables are solved for with the same accuracy: this was not checked in [24], although Mitchell et al. [25] showed that, without due caution, it is possible to obtain numerical solutions for which the temperature is second-order accurate, but the temperature derivatives are only first-order accurate. Furthermore, the actual value of the key controlling dimensionless parameter in such problems, the Stefan number, turns out to affect the efficiency of the iteration scheme given in [24], and therefore a new strategy is required.

In Section 2, we formulate an ablation-type Stefan problem that has been discussed previously in the literature [1], but for which an accurate numerical solution was unavailable; we identify special cases of this problem also [26,27]. In Section 3, we extract important analytical details from the ablation problem; an understanding of these prior to computation turns out to be essential. Section 4 explains how the resulting equations are implemented numerically; as in [24,25], we use the Keller box scheme in tandem with the boundary immobilization method. The results are then presented and discussed in Section 5, and conclusions are drawn in Section 6.

2. Mathematical formulation

We consider a Stefan problem for the variable T, which can be thought of as the dimensionless temperature, that satisfies the heat equation,

$$\frac{\partial T}{\partial t} = \frac{\partial^2 T}{\partial x^2}, \quad s(t) < x < \infty, \tag{1}$$

subject to the boundary conditions

$$T \to -1, \quad \text{as } x \to \infty \tag{2}$$

$$T = 0, \qquad \beta \frac{ds}{dt} = 1 + \frac{\partial T}{\partial x}, \quad \text{at } x = s, \tag{3}$$

and the initial conditions

$$T(x, 0) = -1, \qquad s(0) = 0, \tag{4}$$

where $s(t)$ denotes the location of the moving phase-change front, β is a strictly positive constant that corresponds to the reciprocal of the Stefan number and the constant on the right-hand side of (3) represents a heat source. With this formulation, there are two possibilities:

1. $s'(0) < 0$ at $t = 0$, where the prime denotes differentiation with respect to t. The governing equations describe the melting of a block of ice when hot water is thrown over it, where the constant term in the Stefan condition represents a turbulent heat flux [26,27];
2. $s'(0) = 0$. The governing equations constitute a standard ablation model describing the removal of mass from an object by vaporization or other similar erosive processes [4,5]. A characteristic feature is that there is a heating-up phase prior to ablation, during which $s \equiv 0$, so that $T_x = -1$ and $T < 0$ at $x = 0$; only once the material reaches the ablation temperature, i.e. $T = 0$, do we have $s'(t) > 0$ [15,14,1].

Problem 1 can be solved numerically with second-order accuracy for time and space variables using the methods developed in [24,25]; hence, we do not dwell on it here, but will focus instead on problem 2. Note also that the case $s'(0) > 0$, i.e. instantaneous ablation, is not possible, since the heat flux at $x = 0$ is assumed to be finite.

3. Analysis

For Problem 2 there is a preliminary time interval of *a priori* unknown duration, t_1, during which no phase change occurs, although the boundary at $x = 0$ does heat up; this stage ends when $T(0, t) = 0$, i.e. when the ablation temperature

is reached. In the second stage, ablation occurs and material is removed. The equations governing the two stages are as follows:

- *Stage* 1, for $0 \leq t \leq t_1$ and with $s(t) = 0$:

$$\frac{\partial^2 T}{\partial x^2} = \frac{\partial T}{\partial t}, \quad 0 < x < \infty, \tag{5}$$

subject to the boundary conditions

$$\frac{\partial T}{\partial x}(0, t) = -1, \tag{6}$$

$$T \to -1, \quad \text{as } x \to \infty, \tag{7}$$

and the initial condition

$$T(x, 0) = -1. \tag{8}$$

This stage ends when $T(0, t_1) = 0$, which defines t_1. The exact solution to (5)–(8) can be written down as

$$T(x, t) = -1 + 2\sqrt{\frac{t}{\pi}} \exp\left(-\frac{x^2}{4t}\right) - x \operatorname{erfc}\left(\frac{x}{2\sqrt{t}}\right), \tag{9}$$

whence $t_1 = \pi/4$.

- *Stage* 2, with $t > t_1$:

$$\frac{\partial^2 T}{\partial x^2} = \frac{\partial T}{\partial t}, \quad s(t) < x < \infty, \tag{10}$$

subject to the boundary conditions

$$T = 0, \qquad \beta \frac{ds}{dt} = 1 + \frac{\partial T}{\partial x}, \quad \text{at } x = s(t), \tag{11}$$

$$T \to -1, \quad \text{as } x \to \infty, \tag{12}$$

and the initial conditions

$$T(x, t_1) = -1 + 2\sqrt{\frac{t_1}{\pi}} \exp\left(-\frac{x^2}{4t_1}\right) - x \operatorname{erfc}\left(\frac{x}{2\sqrt{t_1}}\right), \qquad s(t_1) = 0. \tag{13}$$

Whilst there is no analytical solution to (10)–(13), headway can nevertheless be made in determining the initial motion of the ablation front in the limit as $t \to t_1^+$. It is convenient to change variables by setting

$$y = x - s, \zeta = t - t_1, \quad T(x, t) = F(y, \zeta). \tag{14}$$

Then, Eqs. (10)–(13) read

$$\frac{\partial^2 F}{\partial y^2} = \frac{\partial F}{\partial \zeta} - \frac{ds}{d\zeta}\frac{\partial F}{\partial y}, \quad 0 < y < \infty, \tag{15}$$

subject to

$$F = 0, \quad \beta \frac{ds}{d\zeta} = 1 + \frac{\partial F}{\partial y}, \text{ at } y = 0, \tag{16}$$

$$F \to -1, \quad \text{as } y \to \infty, \tag{17}$$

$$F(y, t_1) = -1 + 2\sqrt{\frac{t_1}{\pi}} \exp\left(-\frac{y^2}{4t_1}\right) - y \operatorname{erfc}\left(\frac{y}{2\sqrt{t_1}}\right), \qquad s(t_1) = 0. \tag{18}$$

Next, we assume that s has the form [28]

$$s \sim \lambda \zeta^{\alpha} + O(\zeta^{\alpha}), \tag{19}$$

where α and λ are positive constants that are to be determined; here, it is evident, as in [28], that $\alpha > 1$, since the right-hand side of the second equation in (16) vanishes as $t \to t_1^+$. Using (19) for s in (15), we consider the solution to

$$F_{\zeta} - \lambda\alpha\zeta^{\alpha-1} F_y = F_{yy}, \quad 0 < y < \infty, \tag{20}$$

subject to the boundary conditions

$$F(0, \zeta) = 0, \quad F \to -1 \text{ as } y \to \infty, \tag{21}$$

and the initial condition

$$F(y,0) = F_o(y), \tag{22}$$

where $F_o(0) = 0$ and $F_o(\infty) = -1$. For the case when $\lambda = 0$, a closed-form expression in integral form is given by Carslaw & Jaeger [29]. Their analysis, which is based on the use of Fourier transforms defined for $-\infty < y < \infty$, can be exploited here even when $\lambda \neq 0$; we omit the majority of the details and quote the solution for F as

$$F(y,\zeta) = \frac{1}{2}\sqrt{\frac{1}{\pi\zeta}}\int_0^\infty F_o(y')\left\{\exp\left(-\frac{(y+\lambda\zeta^\alpha - y')^2}{4\zeta}\right) - \exp\left(-\frac{(y-\lambda\zeta^\alpha + y')^2}{4\zeta}\right)\right\} dy'. \tag{23}$$

Now, setting $\phi = (y' - \lambda\zeta^\alpha)/2\zeta^{1/2}$, we have

$$(F_y)_{y=0} = 2\sqrt{\frac{1}{\pi\zeta}}\int_{-\frac{1}{2}\lambda\zeta^{\alpha-1/2}}^\infty F_o(\Phi)\,\phi e^{-\phi^2}\,d\phi, \tag{24}$$

where $\Phi = 2\phi\sqrt{\zeta} + \lambda\zeta^\alpha$. Expanding F_o as

$$F_o(\Phi) \approx F_o(0) + \Phi F_{oy}(0) + \frac{\Phi^2}{2}F_{oyy}(0) + O\left(\Phi^3\right), \tag{25}$$

and using the fact that $F_o(0) = 0$, means that (24) becomes

$$(F_y)_{y=0} = 2\sqrt{\frac{1}{\pi\zeta}}F_{oy}(0)\int_{-\lambda\zeta^{\alpha-1/2}/2}^\infty \Phi\phi e^{-\phi^2}\,d\phi + \sqrt{\frac{1}{\pi\zeta}}F_{oyy}(0)\int_{-\lambda\zeta^{\alpha-1/2}/2}^\infty \Phi^2\phi e^{-\phi^2}\,d\phi + \cdots. \tag{26}$$

Calculating these integrals leads to the expression

$$\begin{aligned}(F_y)_{y=0} = {} & F_{oy}(0)\mathrm{erfc}\left(-\frac{\lambda\zeta^{\alpha-1/2}}{2}\right) \\ & + F_{oyy}(0)\left[2\sqrt{\frac{\zeta}{\pi}}\left(1+\frac{\lambda^2\zeta^{2\alpha-1}}{4}\right)\exp\left(-\frac{\lambda^2\zeta^{2\alpha-1}}{4}\right) + \lambda\zeta^\alpha\mathrm{erfc}\left(-\frac{\lambda\zeta^{\alpha-1/2}}{2}\right)\right].\end{aligned} \tag{27}$$

If we expand (27) for small ζ, we obtain

$$(F_y)_{y=0} \approx F_{oy}(0)\left(1 + \frac{\lambda}{2}\zeta^{\alpha-1/2} + \cdots\right) + 2\sqrt{\frac{\zeta}{\pi}}F_{oyy}(0) + \cdots. \tag{28}$$

Since $\alpha > 1$, we must have

$$(F_y)_{y=0} - F_{oy}(0) \sim \frac{2}{\sqrt{\pi}}F_{oyy}(0)\zeta^{1/2}. \tag{29}$$

Hence, from the Stefan condition given in the second equation in (16), we have at leading order in ζ,

$$\beta\alpha\lambda\zeta^{\alpha-1} = \frac{2}{\sqrt{\pi}}F_{oyy}(0)\zeta^{1/2}, \tag{30}$$

from which we can deduce that $\alpha = 3/2$ and so

$$\lambda = \frac{4F_{oyy}(0)}{3\beta\sqrt{\pi}}. \tag{31}$$

Finally, using (18), we note that $F_{oyy}(0) = 1/\sqrt{\pi t_1}$, whence

$$\lambda = \frac{8}{3\beta\pi^{3/2}}. \tag{32}$$

As a corollary, we note that this result happens to be identical to that derived by Vynnycky & Mitchell [28] for a two-phase Stefan problem that is of relevance in the continuous casting of metals [30,31], even though there is no ablation there.

4. Numerical method

4.1. Discussion

Here, we will once again focus on developing a scheme centred on the Keller Box method, in tandem with transformed variables. We begin by immobilizing the moving boundary by using the variables

$$y = x - s, \quad T(x,t) = F(y,t). \tag{33}$$

With this transformation, Eqs. (1)–(4) become

$$\frac{\partial^2 F}{\partial y^2} = \frac{\partial F}{\partial t} - \frac{ds}{dt}\frac{\partial F}{\partial y}, \quad 0 < y < \infty; \tag{34}$$

$$F \to -1, \quad \text{as } y \to \infty; \tag{35}$$

at $y = 0$,

$$\begin{cases} \dfrac{\partial F}{\partial y} = -1, & \text{if } s = 0 \\ \dfrac{\partial F}{\partial y} = -1 + \beta\dfrac{ds}{dt}, F = 0, & \text{if } s > 0; \end{cases} \tag{36}$$

$$F(y, 0) = -1, \qquad s(0) = 0. \tag{37}$$

For $0 \le t \le t_1$, we will have $s \equiv 0$, and therefore a fixed-boundary problem. Despite this, two issues still arise:

(A) What will be the numerical accuracy of the solution?
(B) Will the numerical scheme be able to capture the analytical value of t_1?

Some guidance as regards (A) is given in [25], where it was found by numerical experimentation that solving in y and t variables would not give second-order accuracy for either the dependent variable or its derivative with respect to y. The reason for is that there is an inconsistency, or discontinuity, for F_y near (0,0), since

$$F_y(y, 0) \to 0 \quad \text{as } y \to 0, \qquad F_y(0, t) = -1 \quad \text{as } t \to 0; \tag{38}$$

note, however, that there is no inconsistency for F, since

$$F(y, 0) \to -1 \quad \text{as } y \to 0, \qquad F(0, t) = -1 \quad \text{as } t \to 0. \tag{39}$$

To avoid this difficulty, we must make a further transformation. Setting

$$\xi = y/\sqrt{t}, \tau = \sqrt{t}, \quad F(y, t) = -1 + \tau H(\xi, \tau), \tag{40}$$

Eqs. (34)–(36) become

$$\frac{\partial^2 H}{\partial \xi^2} = \frac{1}{2}\left(H + \tau\frac{\partial H}{\partial \tau}\right) - \frac{1}{2}\left(\xi + \frac{ds}{d\tau}\right)\frac{\partial H}{\partial \xi}, \quad 0 < \xi < \infty, \tag{41}$$

$$H \to 0, \quad \text{as } \xi \to \infty, \tag{42}$$

and, at $\xi = 0$,

$$\begin{cases} \dfrac{\partial H}{\partial \xi} = -1, & \text{if } s = 0 \\ \dfrac{\partial H}{\partial \xi} = -1 + \dfrac{\beta}{2\tau}\dfrac{ds}{d\tau}, H = 1/\tau, & \text{if } s > 0. \end{cases} \tag{43}$$

To obtain a starting solution, we consider the limit as $\tau \to 0$; here (41) reduces to

$$\frac{d^2 H}{d\xi^2} = \frac{1}{2}H - \frac{\xi}{2}\frac{dH}{d\xi}, \tag{44}$$

which can be solved along with boundary conditions (42) and (43) to give

$$H(\xi) = \frac{2}{\sqrt{\pi}}e^{-\xi^2/4} - \xi\,\text{erfc}\left(\frac{\xi}{2}\right). \tag{45}$$

This gives the initial condition for the discretization scheme. Note also that solving in terms of t, rather than τ, will lead to a scheme that is not second-order accurate for the temperature derivative, as demonstrated by Mitchell et al. [25] for a similar problem. As regards (B), it is evident that, without devising a special algorithm that is able to seek out the true value of t_1, it will not be possible to find it to within a known accuracy. Since this appears to constitute a substantial additional body of work, and since our focus is on obtaining numerical solutions for the ablation phase, we defer it to future work; nevertheless, we will explore the implications of integrating beyond $\tau = \tau_1 \left(:= t_1^{1/2}\right)$ using the same variables as for $\tau \le \tau_1$, to determine whether it can, after all, provide a viable numerical solution for the ablation phase.

Consider now the solution for $t > t_1$; for this, we will use the analytical solution that is available for $t \le t_1$ as the basis for an initial condition for the ablation phase. One possibility would be to use

$$\zeta = x - s(t), \qquad \bar{\tau} = t - t_1,$$

as independent variables, leading to

$$\frac{\partial^2 F}{\partial \zeta^2} = \frac{\partial F}{\partial \bar{\tau}} - \frac{ds}{d\bar{\tau}}\frac{\partial F}{\partial \zeta}, \quad 0 < \zeta < \infty, \tag{46}$$

$$F \to -1, \quad \text{as } \zeta \to \infty, \tag{47}$$

$$F = 0, \quad \beta\frac{ds}{d\bar{\tau}} = 1 + \frac{\partial F}{\partial \zeta}, \text{ at } \zeta = 0, \tag{48}$$

$$F(\zeta, 0) = -1 + 2\sqrt{\frac{t_1}{\pi}}\exp\left(-\frac{\zeta^2}{4t_1}\right) - \zeta\,\text{erfc}\left(\frac{\zeta}{2\sqrt{t_1}}\right), \qquad s(0) = 0. \tag{49}$$

With this formulation, we see that there will be no inconsistency for F or F_ζ near $\zeta = 0$, $\bar{\tau} = 0$, since

$$F(\zeta, 0) \to 0 \quad \text{as } \zeta \to 0, \qquad F(0, \bar{\tau}) \to 0 \quad \text{as } \bar{\tau} \to 0, \tag{50}$$

$$F_\zeta(\zeta, 0) \to -1 \quad \text{as } \zeta \to 0, \qquad F_\zeta(0, \bar{\tau}) \to -1 \quad \text{as } \bar{\tau} \to 0; \tag{51}$$

hence, we might believe that this formulation will lead to second-order accuracy for all variables. A drawback, however, is that powers of $\bar{\tau}^{1/2}$ will appear – since $ds/d\bar{\tau} \sim \bar{\tau}^{1/2}$ initially – which is known to lead to less than second-order accuracy for the derivative [25]. To avoid this, we might use instead

$$\zeta = x - s(t), \qquad \bar{\tau} = \sqrt{t - t_1},$$

to obtain

$$2\bar{\tau}\frac{\partial^2 F}{\partial \zeta^2} = \frac{\partial F}{\partial \bar{\tau}} - \frac{ds}{d\bar{\tau}}\frac{\partial F}{\partial \zeta}, \quad 0 < \zeta < \infty, \tag{52}$$

$$F \to -1, \quad \text{as } \zeta \to \infty, \tag{53}$$

$$F = 0, \qquad \frac{\beta}{2\bar{\tau}}\frac{ds}{d\bar{\tau}} = 1 + \frac{\partial F}{\partial \zeta}, \quad \text{at } \zeta = 0, \tag{54}$$

$$F(\zeta, 0) = -1 + 2\sqrt{\frac{t_1}{\pi}}\exp\left(-\frac{\zeta^2}{4t_1}\right) - \zeta\,\text{erfc}\left(\frac{\zeta}{2\sqrt{t_1}}\right), \qquad s(0) = 0. \tag{55}$$

This removes the powers of $\bar{\tau}^{1/2}$, and there are no inconsistencies near $\zeta = 0$, $\bar{\tau} = 0$, but $\bar{\tau}$ multiplies the highest order derivative in (52). Since the integration has to be started at $\bar{\tau} = 0$, this form is inappropriate for numerical implementation in the context of order-of-accuracy studies, which rely on establishing the behaviour of the numerical scheme as the size of the time step is decreased to zero.

Instead, we try to rewrite the equations in a way such that there *is* an inconsistency and so that there are no fractional powers of $\bar{\tau}$, the rationale being that we have already demonstrated we are able to obtain a numerical scheme that is second-order accurate in all variables under such conditions [25]. First of all, observe that there *will* be an inconsistency in $F_{\zeta\zeta}$ in (46)–(49) near $\zeta = 0$, $\bar{\tau} = 0$, since

$$F_{\zeta\zeta}(\zeta, 0) \to 2\left(\frac{t_1}{\pi}\right)^{1/2} \quad \text{as } \zeta \to 0, \qquad F_{\zeta\zeta}(0, \bar{\tau}) \to 0 \quad \text{as } \bar{\tau} \to 0;$$

so, we reformulate these in terms of $\mathcal{F} := F_\zeta$. Thus,

$$\frac{\partial^2 \mathcal{F}}{\partial \zeta^2} = \frac{\partial \mathcal{F}}{\partial \bar{\tau}} - \frac{ds}{d\bar{\tau}}\frac{\partial \mathcal{F}}{\partial \zeta}, \quad 0 < \zeta < \infty, \tag{56}$$

$$\mathcal{F} \to 0, \quad \text{as } \zeta \to \infty, \tag{57}$$

$$\frac{\partial \mathcal{F}}{\partial \zeta} = -\frac{ds}{d\bar{\tau}}\mathcal{F}, \qquad \beta\frac{ds}{d\bar{\tau}} = 1 + \mathcal{F}, \quad \text{at } \zeta = 0, \tag{58}$$

$$\mathcal{F}(\zeta, 0) = -\text{erfc}\left(\frac{\zeta}{2\sqrt{t_1}}\right), \qquad s(0) = 0. \tag{59}$$

Note that the first equation in (58) has been obtained by observing that since $F = 0$ at $\zeta = 0$, it follows that $F_{\bar{\tau}} = 0$ at $\zeta = 0$; then, we use (46). Now, set

$$\mathcal{F}(\zeta, \bar{\tau}) = g(\zeta) + \hat{H}(\zeta, \bar{\tau}), \tag{60}$$

where $g(\zeta) = -\text{erfc}\left(\zeta/[2\sqrt{t_1}]\right)$, giving

$$\frac{\partial^2 \hat{H}}{\partial \zeta^2} = \frac{\partial \hat{H}}{\partial \bar{\tau}} - \frac{ds}{d\bar{\tau}}\frac{\partial \hat{H}}{\partial \zeta} + g_1(\zeta, \bar{\tau}), \quad 0 < \zeta < \infty, \tag{61}$$

$$\hat{H} \to 0, \quad \text{as } \zeta \to \infty, \tag{62}$$

$$\frac{\partial \hat{H}}{\partial \zeta} = -\frac{ds}{d\bar{\tau}}\hat{H} + g_2(\bar{\tau}), \qquad \beta\frac{ds}{d\bar{\tau}} = \hat{H}, \quad \text{at } \zeta = 0, \tag{63}$$

$$\hat{H}(\zeta, 0) = 0, \qquad s(0) = 0, \tag{64}$$

with

$$g_1(\zeta, \bar{\tau}) = -\frac{ds}{d\bar{\tau}}g'(\zeta) - g''(\zeta), \qquad g_2(\bar{\tau}) = -\frac{ds}{d\bar{\tau}}g(0) - g'(0).$$

In view of the inconsistency in $\hat{H}_\zeta$ and the appearance of $\bar{\tau}^{1/2}$ through $ds/d\bar{\tau}$, we set

$$\hat{H} = \bar{\tau}^{1/2}\bar{H}(\eta, \tilde{\tau}), \quad \eta = \zeta/\bar{\tau}^{1/2}, \tilde{\tau} = \bar{\tau}^{1/2}, \tag{65}$$

so that (61)–(64) become

$$\frac{\partial^2 \bar{H}}{\partial \eta^2} = \frac{1}{2}\bar{H} + \frac{1}{2}\tilde{\tau}\frac{\partial \bar{H}}{\partial \tilde{\tau}} - \frac{1}{2}\left(\eta + \frac{ds}{d\tilde{\tau}}\right)\frac{\partial \bar{H}}{\partial \eta} + \tilde{\tau}g_1(\eta\tilde{\tau}, \tilde{\tau}), \quad 0 < \eta < \infty, \tag{66}$$

$$\bar{H} \to 0, \quad \text{as } \eta \to \infty, \tag{67}$$

$$\frac{\partial \bar{H}}{\partial \eta} = -\frac{1}{2}\frac{ds}{d\tilde{\tau}}\bar{H} + g_2(\tilde{\tau}), \qquad \beta\frac{ds}{d\tilde{\tau}} = 2\tilde{\tau}^2\bar{H}, \quad \text{at } \eta = 0, \tag{68}$$

$$\bar{H}(\eta, 0) = 0, \qquad s(0) = 0. \tag{69}$$

Note here the significance of the transformations in (60) and (65): they ensure that a starting similarity solution can be found to (66)–(69), as shown below. Without the substitution, it would be necessary to treat (56)–(59) numerically using a double-deck integration scheme, as implemented in [32] and discussed in [25], which is an altogether more cumbersome task.

Now, in the limit as $\tilde{\tau} \to 0$, we have

$$\frac{d^2 \bar{H}}{d\eta^2} = \frac{1}{2}\bar{H} - \frac{\eta}{2}\frac{d\bar{H}}{d\eta}, \quad 0 < \eta < \infty, \tag{70}$$

subject to

$$\bar{H} \to 0, \quad \text{as } \eta \to \infty \tag{71}$$

$$\frac{\partial \bar{H}}{\partial \eta} = g_2(0), \quad \text{at } \eta = 0; \tag{72}$$

once this is solved, we can find the initial behaviour of s. Thus,

$$\bar{H} = -\frac{\eta}{(\pi t_1)^{1/2}} + \frac{2}{\pi t_1^{1/2}}\left(e^{-\eta^2/4} + \frac{\sqrt{\pi}}{2}\eta\,\text{erf}\left(\frac{\eta}{2}\right)\right), \tag{73}$$

whence

$$\beta\frac{ds}{d\tilde{\tau}} \sim \left(\frac{2}{\pi t_1^{1/2}}\right)\tilde{\tau}^2, \tag{74}$$

leading to

$$s \sim \left(\frac{8}{3\beta\pi^{3/2}}\right)\tilde{\tau}^3, \tag{75}$$

which agrees with the result obtained in Section 3.

Whilst the formulation given by Eqs. (66)–(69) is, without doubt, superior to those given by (46)–(49) and (52)–(55), there are some further improvements that can be made. As it stands, the formulation does not guarantee that the behaviour given by Eq. (75) will be reproduced. To this end, we introduce

$$s = \tilde{\tau}^3 S,$$

and rewrite (66)–(69) as, for $0 < \eta < \infty$,

$$\frac{\partial^2 \bar{H}}{\partial \eta^2} = \tfrac{1}{2}\bar{H} + \tfrac{1}{2}\tilde{\tau}\tfrac{\partial \bar{H}}{\partial \tilde{\tau}} - \tfrac{1}{2}\left[\eta + \tilde{\tau}^2\left(3S + \tilde{\tau}\tfrac{dS}{d\tilde{\tau}}\right)\right]\tfrac{\partial \bar{H}}{\partial \eta} + \tilde{\tau} g_1(\eta\tilde{\tau}, \tilde{\tau}), \tag{76}$$

subject to

$$\bar{H} \to 0, \quad \text{as } \eta \to \infty, \tag{77}$$

$$\frac{\partial \bar{H}}{\partial \eta} = -\frac{1}{2}\tilde{\tau}^2\left(3S + \tilde{\tau}\frac{dS}{d\tilde{\tau}}\right)\bar{H} + f_2(\tilde{\tau}), \qquad \beta\left(3S + \tilde{\tau}\frac{dS}{d\tilde{\tau}}\right) = 2\bar{H}, \quad \text{at } \eta = 0, \tag{78}$$

$$\bar{H}(\eta, 0) = 0, \qquad S(0) = \frac{8}{3\beta\pi^{3/2}}. \tag{79}$$

4.2. Discretization schemes

The above discussion leads us to consider the following cases:

(a) Eqs. (34)–(37) for all $t > 0$;
(b) Eqs. (41)–(43) for all $\tau > 0$;
(c) Eqs. (46)–(49) for $\bar{\tau} > 0$;
(d) Eqs. (66)–(69) for $\tilde{\tau} > 0$;
(e) Eqs. (76)–(79) for $\tilde{\tau} > 0$.

In the interest of brevity, we indicate how the Keller Box scheme is applied to case (a); the details for the other cases follow analogously. First, it is convenient to re-write (34) as a system of two first-order equations by setting $V = \frac{\partial F}{\partial y}$. This gives

$$\frac{\partial F}{\partial y} = V, \qquad \frac{\partial V}{\partial y} = \frac{\partial F}{\partial t} - \frac{ds}{dt}V, \tag{80}$$

with boundary conditions

$$\begin{cases} V = -1, & \text{if } s = 0 \\ V = -1 + \beta\dfrac{ds}{dt}, F = 0, & \text{if } s > 0 \end{cases} \quad \text{at } y = 0, \tag{81}$$

$$F \to -1, \quad \text{as } y \to \infty. \tag{82}$$

The initial conditions are

$$F(y, 0) = -1, \qquad V(y, 0) = 0. \tag{83}$$

For a general dependent variable C and general independent variables X and Y, we define the following finite difference operators:

$$\mu_X C_{i+\frac{1}{2}}^{n+\frac{1}{2}} = \frac{C_{i+\frac{1}{2}}^{n+1} + C_{i+\frac{1}{2}}^{n}}{2}, \qquad \delta_X C_{i+\frac{1}{2}}^{n+\frac{1}{2}} = \frac{C_{i+\frac{1}{2}}^{n+1} - C_{i+\frac{1}{2}}^{n}}{\Delta X}, \tag{84}$$

$$\mu_Y C_{i+\frac{1}{2}}^{n+\frac{1}{2}} = \frac{C_{i+1}^{n+\frac{1}{2}} + C_{i}^{n+\frac{1}{2}}}{2}, \qquad \delta_Y C_{i+\frac{1}{2}}^{n+\frac{1}{2}} = \frac{C_{i+1}^{n+\frac{1}{2}} - C_{i}^{n+\frac{1}{2}}}{\Delta Y}. \tag{85}$$

With $X = t$, $Y = y$, the box scheme applied to Eqs. (80) therefore gives, for $n = 0, 1, 2, \ldots$,

$$\mu_t \delta_y F_{i+\frac{1}{2}}^{n+\frac{1}{2}} = \mu_t \mu_y V_{i+\frac{1}{2}}^{n+\frac{1}{2}}, \tag{86}$$

$$\mu_t \delta_y V_{i+\frac{1}{2}}^{n+\frac{1}{2}} = \mu_y \delta_t F_{i+\frac{1}{2}}^{n+\frac{1}{2}} - \delta_t s^{n+\frac{1}{2}} \mu_t \mu_y V_{i+\frac{1}{2}}^{n+\frac{1}{2}}, \tag{87}$$

which holds for $i = 1, \ldots, I-1$. Note that $s^{n+\frac{1}{2}} = (s^{n+1} - s^n)/\Delta t$, analogous to the operators defined in (86) and (87). Boundary conditions (81) and (82) are

$$\begin{cases} V_0^n = -1, & \text{if } s^n = 0 \\ \mu_t V_0^{n+\frac{1}{2}} = -1 + \beta\,\delta_t s^{n+\frac{1}{2}}, F_0^n = 0, & \text{if } s^n > 0, \end{cases} \tag{88}$$

$$F_I^n = -1, \tag{89}$$

respectively. Using (83), the initial conditions are written as

$$F_i^0 = -1, \qquad V_i^0 = 0. \tag{90}$$

In the above, a uniform mesh is used for the space variable. In practice, a finite computational domain of extent y_∞ is chosen, although this must be large enough to ensure that correct asymptotic behaviour as $y \to \infty$ is captured; since F known to decay exponentially as $y \to \infty$, $y_\infty = 10$ proves to be adequate enough.

For cases (a) and (b), the algorithm must monitor whether or not ablation has actually begun, in order to implement the switch in boundary condition (88). This is done by checking the value of F_0^n: the time corresponding to the first value of n for which $F_0^n > 0$, denoted by t^n, is then considered as the numerical value of t_1.

A further detail is that Eq. (87) involves s^{n+1}, so that the overall system of equations is nonlinear; to handle this, it is necessary to iterate on s^{n+1}. It is updated using the Stefan condition (88) until some desired tolerance, ε, is reached [24]; denoting by $s_{(m)}^{n+1}$ the value for s^{n+1} after m iterations, the convergence criterion used is

$$\left| s_{(m+1)}^{n+1} - s_{(m)}^{n+1} \right| < \varepsilon. \tag{91}$$

There is, however, an additional subtlety regarding how to commence iterations in s at a new value of n. The strategy used in [24] was simply to set $s_{(1)}^{n+1} = s^n$, with $s_{(m)}^{n+1}$ subsequently coming from the Stefan condition, i.e. a relaxation-type procedure. Unfortunately, the number of iterations required to fulfil (91) was found to increase dramatically for low values of β ($\lesssim 0.1$). A more robust strategy was found from using (88) directly, by setting

$$s_{(1)}^{n+1} = s^n + \left(V_0^n + V_{0,(1)}^{n+1} + 2 \right) / \beta,$$

where $V_{0,(1)}^{n+1}$ where is the value of V_0^{n+1} on the first iteration. Ultimately, never more than 10 iterations in s were necessary to satisfy (91); for all runs, we set $\varepsilon = 10^{-13}$.

4.3. Order of accuracy

We will also wish to determine the order of accuracy of schemes (a)–(e). We start this discussion by considering a sequence ΔY_k where

$$\Delta Y_k = 2^{-k} \Delta Y_0, \quad k = 1, 2, \ldots,$$

and we denote the space coordinates of meshes associated with this sequence by

$$Y_{i,k} = i \Delta Y_k, \quad i = 0, 1, \ldots, I_k, k = 0, 1, 2, \ldots,$$

where

$$I_k = 2^k I_0, \quad k = 1, 2, \ldots.$$

As discussed in [33], for a general numerical solution $F_{2^k i}^n$ and corresponding exact solution $f(Y_{i,k}, t^n)$ at the nth time step, t^n, the error and corresponding order of convergence, $E_{F,k}^n$ and $p_{F,k}$ respectively, are given by

$$E_{F,k}^n = \left(\Delta Y_k \sum_{i=0}^{I_0} \left(f(Y_{i,0}, t^n) - F_{2^k i}^n \right)^2 \right)^{1/2}, \qquad p_{F,k} = \frac{\ln(E_{F,k}^n / E_{F,k+1}^n)}{\ln 2}, \tag{92}$$

for $k = 0, 1, 2, \ldots$. In order to be able to make use of (92), it is necessary that an exact solution is known. However, as demonstrated in [24], it turns out to be possible to estimate the order of accuracy even when an exact solution is not known. Instead of $E_{F,k}^n$ in (92), for a general numerical solution F_i^n we define

$$\bar{E}_{F,k}^n = \left(\sum_{i=0}^{I_0} \left(F_{2^k i}^n - F_{2^{k-1} i}^n \right)^2 \right)^{1/2}, \qquad \bar{p}_F = \ln(\bar{E}_{F,k}^n / \bar{E}_{F,k+1}^n) / \ln 2, \tag{93}$$

for $k = 1, 2, \ldots$. In cases where an exact solution was known, Mitchell & Vynnycky [24] showed that $p_F = \bar{p}_F$, where

$$p_F = \lim_{k \to \infty} p_{F,k}, \qquad \bar{p}_F = \lim_{k \to \infty} \bar{p}_{F,k}.$$

Furthermore, Mitchell et al. [25] demonstrated that it was also possible to apply this idea to the spatial derivative of F and s; thus, we set, for $k = 0, 1, 2, \ldots$,

$$E_{V,k}^n = \left(\Delta Y_k \sum_{i=0}^{I_0} \left(v(Y_{i,0}, t^n) - V_{2^k i}^n \right)^2 \right)^{1/2}, \qquad p_{V,k} = \frac{\ln(E_{V,k}^n / E_{V,k+1}^n)}{\ln 2}, \tag{94}$$

$$E_{s,k}^n = \left| s_k^n - s(t^n) \right|, \quad k = 0, 1, 2, \ldots, \qquad p_{s,k} = \frac{\ln(E_{s,k}^n / E_{s,k+1}^n)}{\ln 2}, \tag{95}$$

Table 1
Order of accuracy for schemes (a) and (b) for a sequence of meshes at $t = 0.5$ and $\tau = 0.5$, prior to the onset of ablation. Note that $\beta = 1$ and $\Delta t = \Delta\tau = 0.02$ for $k = 0$.

		Δy, $\Delta\xi$ (k)				
		2/5 (1)	1/5(2)	1/10(3)	1/20(4)	1/40(5)
(a)	p_F	1.45309	1.26544	1.14098	1.07156	1.03582
	$\bar{p}_F$	–	1.22600	1.11637	1.05584	1.02697
	p_V	1.56605	1.42286	1.28764	1.17917	1.10301
	$\bar{p}_V$	–	2.38646	1.65124	0.54662	0.77956
(b)	p_F	2.03818	2.01971	2.01000	2.00504	2.00253
	$\bar{p}_F$	–	2.00096	2.00023	2.00005	2.00001
	p_V	2.01004	2.00248	2.00062	2.00015	2.00004
	$\bar{p}_V$	–	2.01255	2.00311	2.00077	2.00019

Table 2
Order of accuracy for schemes (a) and (b) for a sequence of meshes at $t = 1$ and $\tau = 1$, after the onset of ablation. Note that $\beta = 1$ and $\Delta t = \Delta\tau = 0.02$ for $k = 0$.

		Δy, $\Delta\xi$ (k)			
		1/5 (2)	1/10(3)	1/20(4)	1/40(5)
(a)	$\bar{p}_F$	3.14710	0.67092	1.38042	−0.21495
	$\bar{p}_V$	0.74102	1.86874	2.66553	−0.26774
	$\bar{p}_s$	2.57378	0.99755	0.99695	−0.58758
(b)	$\bar{p}_F$	1.93045	3.14213	1.11864	−0.41251
	$\bar{p}_V$	1.14907	1.57443	−1.07917	4.07042
	$\bar{p}_s$	−0.73538	4.86186	2.03173	−3.73584

where $v = \partial f/\partial y$, and

$$\bar{E}^n_{V,k} = \left(\sum_{i=0}^{I_0} \left(V^n_{2^k i} - V^n_{2^{k-1} i}\right)^2\right)^{1/2}, \qquad \bar{p}_{V,k} = \ln(\bar{E}^n_{V,k}/\bar{E}^n_{V,k+1})/\ln 2 \tag{96}$$

$$\bar{E}^n_{s,k} = \left|s^n_k - s^n_{k-1}\right|, \quad k = 1, 2, \ldots, \qquad \bar{p}_{s,k} = \ln(\bar{E}^n_{s,k}/\bar{E}^n_{s,k+1})/\ln 2, \tag{97}$$

for $k = 1, 2, \ldots$.

5. Results

5.1. Cases (a) and (b)

First, we consider the numerical accuracy of schemes (a) and (b). Table 1 compares the relevant values of p and $\bar{p}$ for a sequence of progressively finer meshes at arbitrary values of the time-like variable prior to the start of ablation. The data suggests that scheme (a) gives first-order accuracy for the temperature and the heat flux, although it appears that even further mesh refinement would be necessary in order to obtain values of p closer to 1; for scheme (b), on the other hand, there is much stronger evidence that we have second-order accuracy in time and space variables for the temperature and the heat flux.

Table 2 gives the corresponding data at arbitrary values of the time-like variable after ablation has started. From this, it is evident that, from the point of view of an order-of-accuracy index, it is not possible to obtain meaningful data for either scheme. This provides strong motivation for considering schemes (c)–(e).

5.2. Cases (c)–(e)

Table 3 compares the relevant values of p for a sequence of progressively finer meshes for schemes (c)–(e) at arbitrary values of the time-like variable after the start of ablation. From this, it is evident that all three schemes give second-order accuracy for the temperature and the location of the moving front; on the other hand, scheme (c) gives first-order accuracy for the heat flux, whereas schemes (d) and (e) give second-order accuracy.

5.3. Summary

The data in Tables 2 and 3 is summarized in Table 4, which shows the index of order of accuracy that is obtained at arbitrary values of the time-like variable after the start of ablation for each of the five schemes. The symbol "X" in the first two rows is used to indicate that no meaningful value for this index can be found for schemes (a) and (b).

Table 3
Order of accuracy for schemes (c)–(e) for a sequence of meshes at $\bar{\tau} = 0.5$ and $\bar{\tau} = 0.5$. Note that $\beta = 1$ and $\Delta\bar{\tau} = \Delta\tilde{\tau} = 0.1$ for $k = 0$.

		$\Delta\zeta, \Delta\eta$ (k)			
		1/8 (2)	1/16(3)	1/32(4)	1/64(5)
(c)	$\bar{p}_F$	1.81790	2.08444	2.06834	2.01811
	$\bar{p}_V$	1.83496	1.56098	1.51582	0.99233
	$\bar{p}_s$	2.01547	2.01338	2.00514	2.00213
(d)	$\bar{p}_F$	2.02198	2.00504	2.00119	2.00028
	$\bar{p}_V$	1.99976	1.98278	1.99210	1.99623
	$\bar{p}_s$	2.04412	2.01095	2.00270	2.00066
(e)	$\bar{p}_F$	2.02198	2.00504	2.00119	2.00028
	$\bar{p}_V$	1.99976	1.98278	1.99210	1.99623
	$\bar{p}_s$	2.05031	2.01234	2.00303	2.00074

Table 4
Order of accuracy for schemes (a)–(e) after the onset of ablation.

	$\bar{p}_F$	$\bar{p}_V$	$\bar{p}_s$
(a)	X	X	X
(b)	X	X	X
(c)	2	1	2
(d)	2	2	2
(e)	2	2	2

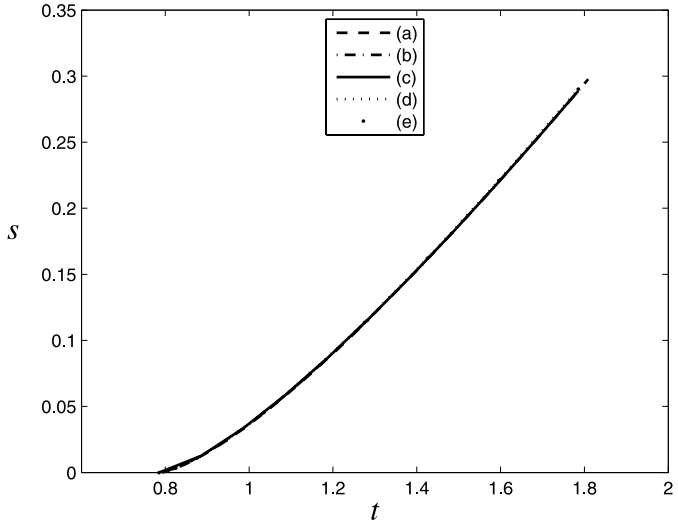

Fig. 1. $s(t)$ vs. t for schemes (a)–(e). The schemes all give the same "working" solutions, although only (c)–(e) are formally accurate.

Although only schemes (c)–(e) can be relied on in a strict numerical sense, it is nonetheless of interest to compare the profiles of s that each of the five schemes gives; this is shown in Fig. 1 and in each case the profile obtained for $k = 4$ has been used. For schemes (a) and (b), ablation starts at $t = 0.7850$ and $t = 0.7832$, respectively, whereas it starts at the analytical value of $\pi/4 \approx 0.7854$ for the other three schemes. From this plot, it is evident that even schemes (a) and (b) can give "working" solutions, even though they are not formally accurate.

6. Conclusions

This paper has considered the so-called boundary immobilization method, in tandem with the Keller box finite-difference scheme, for the numerical solution of one-dimensional ablation-type Stefan problems. An important component of the work was the use of variable transformations that must be built into the numerical algorithm in order to preserve second-order accuracy in both time and space for the temperature and the heat flux. A new analytical finding was that the ablation front, once it forms, moves considerably more slowly than the phase-change front in the classical Stefan problem with isothermal cooling: the relevant time exponents are 3/2 and 1/2, respectively.

There are several possible extensions to this work. Most obviously, it would be desirable to construct a second-order accurate numerical scheme that is able to handle the transition from pre-ablation to ablation; at present, because the issue of how to capture accurately the ablation time was not the focus of this paper, we are unable to retain second-order accuracy after the onset of ablation. Also, we note that the analysis presented here will be a key component in understanding the complete analytical structure of the solution in two-phase moving-boundary problems, for which numerical solutions have recently been obtained [30,31,28,34–36], although not with the level of accuracy we have shown here.

Acknowledgement

The authors acknowledge the support of the Mathematics Applications Consortium for Science and Industry (MACSI, www.macsi.ul.ie) funded by the Science Foundation Ireland Mathematics Initiative Grant 06/MI/005.

References

[1] J.G. Andrews, D.R. Atthey, On the motion of an intensely heated evaporating boundary, J. Inst. Math. Appl. 15 (1975) 59–72.
[2] Y.-K. Chen, F.S. Milos, Ablation and thermal response program for spacecraft heatshield analysis, J. Spacecraft Rockets 36 (3) (1999) 475–483.
[3] A.J. Campbell, M. Humayun, Trace element microanalysis in iron meteorites by laser ablation ICPMS, Anal. Chem. 71 (5) (1999) 939–946.
[4] W.-S. Lin, Steady ablation on the surface of a two-layer composite, Int. J. Heat Mass Transf. 48 (2005) 5504–5519.
[5] A.B. Tayler, Mathematical Models in Applied Mechanics, Oxford University Press, 2001.
[6] W.D. Johnson, The profile of maturity in apline glacial erosion, J. Geology 12 (7) (1904) 569–578.
[7] K. Namenanee, J. McKenzie, E. Kosa, M. Schwab, B. Sunsaneewitayakul, T. Vasavakul, C. Khunnawat, T. Ngarmukos, A new approach for catheter ablation of atrial fibrillation: mapping of the electrophysiologic substrate, J. Amer. College Cardiology 43 (11) (2004) 2044–2053.
[8] H.G. Landau, Heat conduction in a melting solid, Quart. Appl. Math. 8 (1950) 81–94.
[9] T.R. Goodman, Application of integral methods to transient nonlinear heat transfer, Adv. Heat Transf. 1 (1964) 51–122.
[10] T.-F. Zien, Integral solutions of ablation problems with time-tependent heat flux, AIAA J. 16 (1978) 1287–1296.
[11] W.F. Braga, M.B.H. Mantelli, J.L.F. Azevedo, Approximate analytical solution for one-dimensional ablation problem with time-variable heat flux (AIAA 2003-4047), in: AIAA Thermophys. Conference, 2003.
[12] W.F. Braga, M.B.H. Mantelli, J.L.F. Azevedo, Approximate analytical solution for one-dimensional finite ablation problem with constant time heat flux (AIAA 2004-2275), in: AIAA Thermophys. Conference, 2004.
[13] W.F. Braga, M.B.H. Mantelli, J.L.F. Azevedo, Analytical solution for one-dimensional semi-infinite heat transfer problem with convection boundary condition (AIAA 2005-4686), in: AIAA Thermophys. Conference, 2005.
[14] S.L. Mitchell, T.G. Myers, A heat balance integral method for one-dimensional finite ablation, AIAA J. Thermophysics 22 (3) (2008) 508–514.
[15] S.L. Mitchell, T.G. Myers, Application of standard and refined heat balance integral methods to one-dimensional Stefan problems, SIAM Rev. 52 (2010) 57–86.
[16] S.L. Mitchell, Applying the combined integral method to one-dimensional ablation, Appl. Math. Modelling 36 (2012) 127–138.
[17] T.G. Myers, Optimal exponent heat balance and refined integral methods applied to Stefan problems, Int. J. Heat Mass Transf. 53 (2010) 1119–1127.
[18] L. Yang, Y. Zhang, J.K. Chen, An integral approximate solution to ablation of a two-layer composite with a temporal Gaussian heat flux, Heat Transf. Engng. 32 (5) (2011) 418–428.
[19] M. Storti, Numerical modeling of ablation phenomena as two-phase Stefan problems, Int. J. Heat Mass Transf. 38 (15) (1995) 2843–2854.
[20] J. Wang, H. Wang, J. Sun, J. Wang, Numerical simulation of control ablation by transpiration cooling, Heat Mass Transf. 43 (2007) 471–478.
[21] S.K. Wong, A. Walton, Numerical solution of single-phase problem using a fictitious material, Num. Heat Transf. B 35 (1999) 211–223.
[22] B.F. Blackwell, Numerical prediction of one-dimensional ablation using a finite control volume procedure with exponential differencing, Num. Heat Transf. 14 (1988) 17–34.
[23] B.F. Blackwell, R.E. Hogan, One-dimensional ablation using Landau transformation and finite control volume procedure, J. Thermophys. & Heat Transf. 8 (2) (1994) 282–287.
[24] S.L. Mitchell, M. Vynnycky, Finite-difference methods with increased accuracy and correct initialization for one-dimensional Stefan problems, Appl. Math. Comp. 215 (2009) 1609–1621.
[25] S.L. Mitchell, M. Vynnycky, I.G. Gusev, S.S. Sazhin, An accurate numerical solution for the transient heating of an evaporating droplet, Appl. Math. Comp. 217 (2011) 9219–9233.
[26] H.E. Huppert, Phase changes following the initiation of a hot turbulent flow over a cold solid surface, J. Fluid Mech. 198 (1989) 293–319.
[27] J.R. King, D.S. Riley, Asymptotic solutions to the Stefan problem with a constant heat source at the moving boundary, Proc. R. Soc. Lond. Ser. A 456 (2000) 1163–1174.
[28] M. Vynnycky, S.L. Mitchell, On the solution of Stefan problems with delayed onset of phase change, in: Proceedings of the 7th International Conference on Heat Transfer, Fluid Mechanics and Thermodynamics (19–21 July, Antalya, Turkey), 2010, pp. 1404–1410.
[29] H.S. Carslaw, J.C. Jaeger, Conduction of Heat in Solids, Oxford University Press, London, 1947.
[30] J. Åberg, M. Vynnycky, H. Fredriksson, Heat-flux measurements of industrial on-site continuous copper casting and their use as boundary conditions for numerical simulations, Trans. Ind. Inst. Met. 62 (2009) 443–446.
[31] M. Vynnycky, A mathematical model for air-gap formation in vertical continuous casting: the effect of superheat, Trans. Ind. Inst. Met. 62 (2009) 495–498.
[32] M. Vynnycky, Concerning closed-streamline flows with discontinuous boundary conditions, J. Engrg. Math. 33 (1998) 141–156.
[33] J.C. Strikwerda, Finite Difference Schemes and Partial Differential Equations, second ed., Society for Industrial Mathematics, 2004.
[34] A.P. Roday, M.J. Kazmierczak, Analysis of phase-change in finite slabs subjected to convective boundary conditions: part I—melting, Int. Rev. Chem. Eng. (Rapid Communications) 1 (2009) 87–99.
[35] A.P. Roday, M.J. Kazmierczak, Analysis of phase-change in finite slabs subjected to convective boundary conditions: part II—freezing, Int. Rev. Chem. Eng. (Rapid Communications) 1 (2009) 100–108.
[36] A.P. Roday, M.J. Kazmierczak, Melting and freezing in a finite slab due to a linearly decreasing free-stream temperature of a convective boundary condition, Thermal Sci. 2 (2009) 141–153.